

A Novel Back-to-Back Antenna Design with Dual Vertical Polarization for Enhanced Broadband Performance

Saqlain Mehdi¹, Waleed Hanif¹, Hussnain Hameed²

¹ Center of Research Excellence, GC University Faisalabad, Faisalabad, Pakistan

² Department of Electrical Engineering, Adelaide University, Adelaide, Australia

*Corresponding Author: Saqlain Mehdi (Email Address: saqlain.mehdi22@gmail.com)

Received: 04-05-2024 Revised: 18-10-2024 Accepted: 15-12-2024

Abstract— The concept of wireless power transmission was first proposed by Nikola Tesla. He suggested that he could transfer power through the air. The radio waves and microwaves in the air are captured by the antenna and transferred to the destination. The receiver antenna receives the input energy and powers up the system. However, the first rectifying antennas (rectennas) were developed, enabling the conversion of microwave energy into DC power. Rectennas have undergone significant modifications, pushed by the growing demand for Wireless Power transmission and energy generation in many applications, including IoT devices & bio-medical implants. This paper presents the novelty of rectenna design that leverages a planar antenna topology and a high-efficiency rectifier circuit. The design is optimized using a combination of simulation and experimental techniques, significantly improving power conversion efficiency (PCE) and power obtained. The effects of various design parameters, such as antenna geometry, rectifier topology and input power levels, were investigated and optimized for maximum performance. This enhanced rectenna system has a peak power conversion efficiency (PCE) of 70% and a power output of 100 mW, making it compatible for powering low-power electronic devices.

Keywords— energy harvesting, rectenna, wide-band, radio-frequency (RF), energy generation.

I. INTRODUCTION

The rapid enhancement of the Internet of Things (IoT) has led to increased research on wireless sensor networks (WSN). The main challenge is ensuring these sensors are powered efficiently, as billions of wireless sensors require energy solutions. A shift towards energy-autonomous or battery-less systems is inevitable, with promising solutions such as ambient wireless energy harvesting and wireless power transfer (WPT) through periodic charging. [1] One of the most attractive energy harvesting methods is encompassing radiofrequency (RF) energy. This approach utilizes energy from existing RF signals, which are available passively and continuously in all weather conditions. The

Main sources of this energy are RF communication bands, including Wi-Fi (2.4GHz), GSM (2G), UMTS (3G), LTE (4G) and the emerging 5G networks, which operate around 3500 (MHz). As the 5G networks become widespread, this frequency band will contribute significantly to ambient RF energy. [2] [3] [4]

However, the challenge in antenna design for such an energy harvesting system lies in achieving broadband or multiple-band coverage. Several antennas have been proposed for dual-band or tri-band operations to cover various communication bands (e.g., GSM and UMTS). Designs like the broadband cross-dipole Antenna and slotted antennas have been explored for broader bandwidths, targeting frequencies 1.8 GHz to 3.1 GHz. Still, due to the dispersed nature of RF energy across different bands, it isn't easy to design antennas that can cover all frequencies required for communication. [5] [6] [7]

Moreover, the antenna needs to offer wide-angle and multi-polarization capabilities. By combining multiple ports, these designs enhance the harvested RF power for a given area while minimizing matching requirements.

Despite the growing interest in WEH, ambient RF energy is proportionally low, typically in the 40-50 dBm range. This makes it challenging for the energy harvested through WEH to meet the power demands of wireless sensors, requiring Active power supplementation. One remedy is to combine RF energy harvesting with other sources like solar, kinetic and Thermal energy. Alternatively, active wireless Power transfer (WPT) charging can be used to reinforce the harvested energy; It is more reliable and guaranteed in power supply, with less flexibility in terms of frequency. However, combining WEH and WPT into a single antenna design remains challenging. For WEH, broadband or multi-band characteristics are critical, with an omnidirectional radiation pattern preferred to capture from various directions.

Section 2 will cover the design and simulation of this antenna. In contrast, Section 3 will discuss its radiation performance; Section 4 will present the tested reports of both wireless power transmission and reception, validating the antenna's practical application for WEH/WPT systems.



II. ANTENNA CONSTRUCTION & SIMULATION REVIEW

A. Antenna Geometry:

The antenna under review comprises two mirrored microstrip antenna elements: Face 1 and Face 2. The antenna is structured with one layer of metal patches, two dielectric substrates and an aperture-coupled feeding mechanism. The main components include a central driven patch of size $L_{patch} \times W_{patch}$, placed above the upper-layer substrate, flanked by a pair of symmetrically arranged parasitic patches of $L_{para} \times W_{para}$. These patches have the same width and consistency. At the same time, their lengths can be adjusted, and the separation among the driven and parasitic patches is denoted as g_y [8].

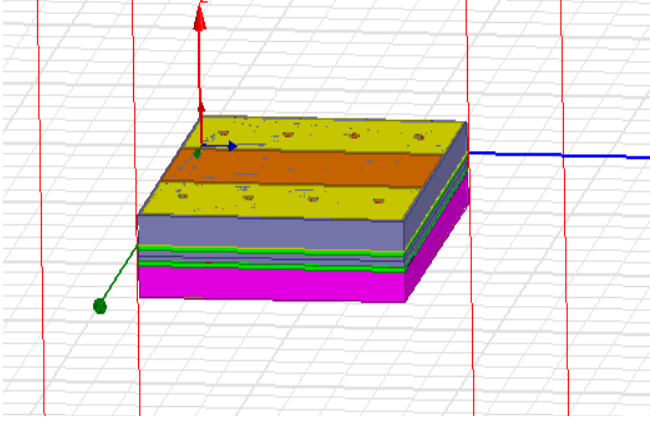


Figure 1: Antenna Design with slotted ground

The ground layer is placed beneath the upper-layer substrate, with a coupled slot etched with dimensions of $L_{slot} \times W_{slot}$. The ground layer is designed to be slightly smaller than the radiator, comprising the driven and parasitic patches. The overall antenna element dimensions are $L_s \times W_s$.

A bi-directional radiation pattern enhances energy distribution, while integrating energy scavenging and directional power transfer in a compact antenna could transform wireless sensor powering.

To connect the micro-address to this, we propose a novel dual-connected micro-strip antenna design that supports 2G/3G/4G/5G communication bands, as well as ISM bands (2.4 GHz and 6.7 GHz), enabling broadband, wide-angle energy generation and directional wireless power transmission.

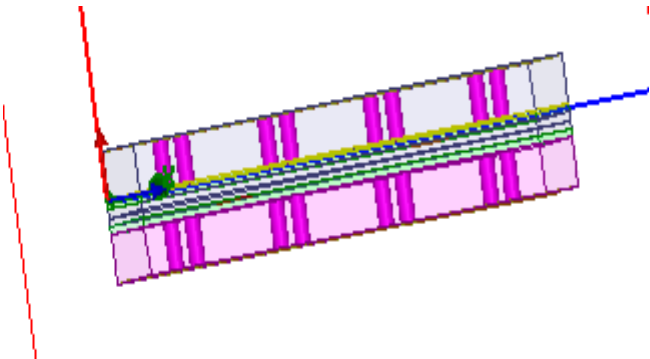


Figure 2 Shorting Vias Connected with respected GND

Parasitic patches are equipped with sets of short vias, with each set containing 4 vias, the separation among these sets is S_1 , while the gap among adjacent vias is S_2 , with the via radius r . The structure is a 3 layered design, where the upper

and lower dielectric substrates are made of F4B material with a relative permittivity of 2.65, a loss tangent of 0.002, and thicknesses h_1 and h_2 , respectively. [1]

Parasitic patches are equipped with short vias, each containing four vias. The separation among these sets S_1 is the figure, while the gap among adjacent vias is S_2 , with the via radius r . The structure is a three-layered design, with the upper and lower dielectric substrates made of F4B material with a relative permittivity of 2.65, a loss tangent of 0.002, and thicknesses h_1 and h_2 , respectively. [8]

The antenna is charged by a micro strip slot-coupled structure, with a 50-ohm micro strip line printed on the bottom layer of the lower substrate having a length of L_s and a W_{feed} . To ensure precise PCB fabrication, the substrate size is slightly larger than the ground layer by 0.6 mm in each direction.

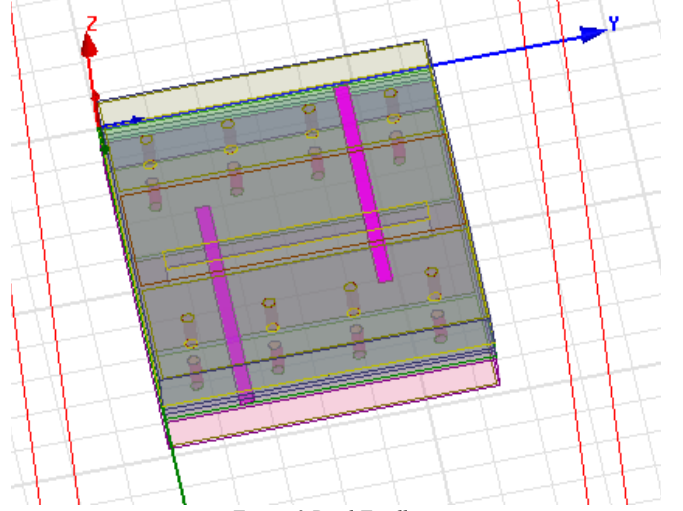


Figure 3 Dual Feedlines

The two antenna elements (Side 1 and Side 2) are combined in a “back-to-back” configuration, sharing a common feed line. The micro strip feeding line is replaced by two strip lines, which are roughly half the characteristic impedance of the micro strip line and opposite in direction. To match the “back-to-back” antenna of 50-ohms, the input impedance is adjusted to approximately 100-ohms.

Table 1 Design Parameters and Dimensions

Parameter	Description	Value (mm)
L_s	Substrate Length (upper and lower)	42.6
W_s	Substrate Width (upper and lower)	32.6
h_1	Upper substrate thickness	3
L_p	Length of driven patch	13.8
W_p	Width of driven patch	32
W_{para}	Width of parasitic patch	32
L_{para}	Length of parasitic patch	13.5
g_y	Space among driven and parasitic patch	0.6
r_s	Via radius	0.6

s2	Space among two sets of shorting vias	27.3
s1	Space among two adjacent of shorting vias	8
Wslot	Slot width	2.8
Lslot	Slot Length	25.9
h2	Lower Substrate thickness	1
Wfl	width of both feedlines	1.4
Lfl	length of both feedlines	30

B. Operational Analysis

The full-wave simulations were conducted using the High-Frequency Structure Simulator (HFSS), and the optimized parameters are summarized in Table 1. The simulated reflection coefficient of the antenna is presented in Fig. The antenna demonstrates resonances at approximately three key frequencies: 3 GHz, 3.4 GHz, 4.2 GHz, 5.2 GHz and 6.7 GHz.

The broadband radiation mechanism of the antenna is explained. To summarize, the “ground mode”, which corresponds to the resonance at 3 GHz, is formed by launching a small ground plane that participates in the radiation. The “driven patch mode”, typically seen in micro strip patch antennas, resonates at 3.2 GHz. Although this resonance should ideally occur at 4.8 GHz, the combination of driven and parasitic patches shifts the resonance to a lower frequency while maintaining the resonance at 3 GHz. [6] [10] The shorting vias further lower the “slot mode” resonance, improving impedance matching and broadening the resonance from 3.0 GHz to 4.2 GHz. This broadband range covers several communication bands, including 2G-GSM1800, 3G-UMTS, ISM-Wi-Fi, 4 G-LTE and 5 G-LMT, enabling efficient RF energy harvesting from these channels. The parasitic patch loading and shorting vias also contribute to a resonance at 6.7 GHz, aligning with another ISM-Wi-Fi band [9].

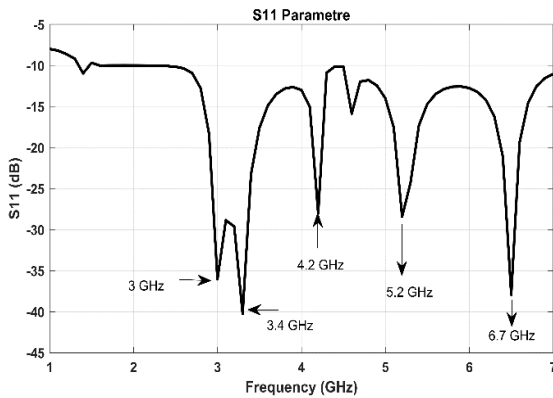


Figure 4 S_{11} Parameters

At 6.7 GHz, the current dispersion on the ground layer and top-plane patches show that the RF energy from the ground is coupled to the top-plane patches, while the driven patch couples' power to the parasitic patches. The current on the parasitic patches uniformly distributed in the same direction, leading to strong radiation from the patch edges. The radiation

. Patterns from both parasitic patches combine to form an efficient radiation pattern at 6.7 GHz.

C. Omni-Directional Approach (Back-to-Back Combination):

For the broadband resonance (Band A), the H-plane radiation pattern is omnidirectional, while the E-plane resembles a dipole pattern along the X-axis. While the beam width is broad, there are nulls at both ends, indicating some non-assessable zones. At lower frequencies, the E-plane directivity increases. To enhance omnidirectionality, Side 1 and 2 are configured in a back-to-back arrangement, sharing the feed line. This alignment connects both elements' E-planes while preserving the omnidirectional nature of the H-plane patterns.

It exhibits improved performance at 6.7 GHz (Band B) due to in-phase superposition, producing a narrow beam. This design allows for better radiation in a specific direction, contributing to enhanced performance at this frequency.

Figure 5 illustrates the simulated 3D radiation patterns and maximum gains at key frequencies. The antenna displays good omnidirectional radiation at Band A, while at Band B, it exhibits bidirectional radiation with strong directivity. The maximum gain is approximately 3.96 dBi.

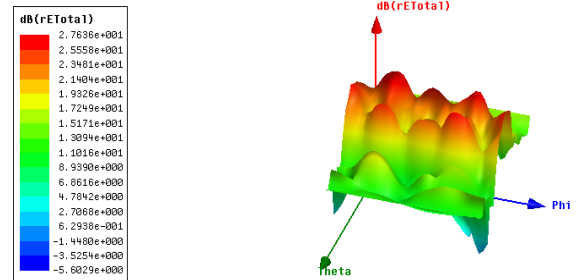
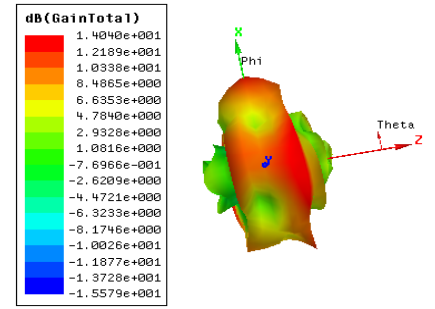


Figure 5 3D and 2D radiation gain



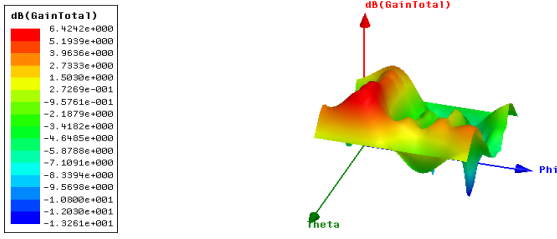


Figure 6: 2D and 3D Plot of rE total

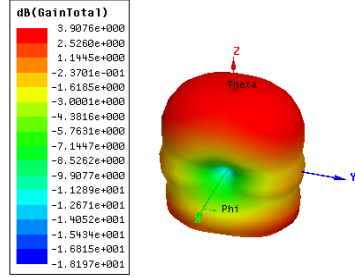


Figure 7: At 6.7GHz

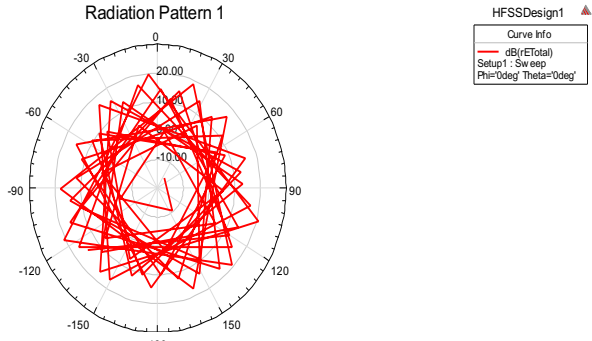


Figure 8: Radiation pattern

III. PROPOSED METHOD

A dual-port simulation model in HFSS assessed the proposed antenna's Wireless Energy Harvesting (WEH) performance. The horn antenna (port-1) acts as the RF source, while the back-to-back antenna (port-2) harvests energy, placed 0.5 meters away. The transmitted power is set to 1W. [10]

Harvesting efficiency (η) is calculated as:

$$\eta = \frac{Pr}{P_{sum}} = \frac{mag(|S_{21}|)^2}{\iint s \vec{E} \times \vec{H} \cdot d\vec{S}}$$

Where Pr is derived from S-parameters, and P_{sum} is from the Pointing vector.

Efficiency was evaluated at various rotational angles (± 15 to ± 75), with peak efficiency at zero rotation. At 2.4 GHz, the harvested power was 10.2 mW with 90% efficiency, at 3.6 GHz, 9.9 mW with 81% efficiency and at 6.7 GHz, 9.2 mW with 70% efficiency. Over the 2-6.7 GHz range, power exceeded 8 mW and efficiency stayed above 80%. The antenna showed excellent angular stability, maintaining 80% efficiency within ± 75 in the 2G-4G range, above 70% within ± 30 at 3.6GHz and above 60% within ± 15 at 6.7GHz.

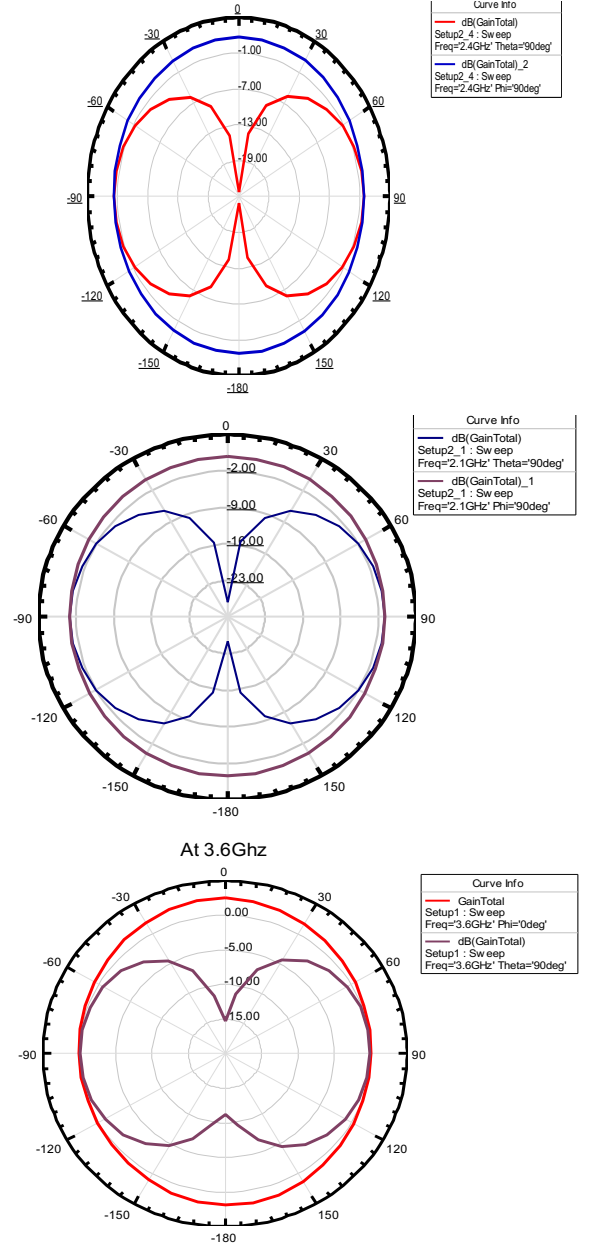


Figure 9: E and H plane at 3GHz, 4.2GHz and 6.7GHz respectively.

IV. CONCLUSION

These results reflect the antenna's omnidirectional nature at lower frequencies and directional behaviour at higher frequencies, making the 6.7 GHz band suitable for directional Wireless Power Transfer (WPT).

In real-world testing, the maximum harvested power at 2.4 GHz was -8.5 dBm, 1 dB lower than the ideal value due to minor test environment losses. Power at other frequencies ranged from -9 dB to -10 dB. Confirming broad performance.

ACKNOWLEDGMENT

The authors extend their sincere gratitude to the Computer Network Laboratory, Department of Electrical Engineering, GC University Faisalabad, for providing a supportive research environment and access to advanced computational resources, which enabled the successful execution of this study.

FUNDING STATEMENT

The author(s) received no specific funding for this study.

CONFLICTS OF INTEREST

The authors declare no conflicts of interest to report regarding the present study.

REFERENCES

- [1] H. Y. H. L. Y. Z. A. L. L. PEI ZHANG, "Back-to-Back Micro strip Antenna Design for Broadband Wide-Angle RF Energy Harvesting and Dedicated Wireless Power Transfer," no. July 2020, p. 8, 2020.
- [2] Y. Souto and B. Filho, "Multiband rectenna for radio frequency energy harvesting applied to wireless sensor network," 2023.
- [3] T. Maruyama, M. Nakatsugawa, N. Suematsu, M. Motoyoshi and Q. Chen, "Novel Design of Rectenna Array Using Metasurface for IoT," 2021.
- [4] T. D. Ha, X. Nie, H. Bağcı, D. Erricolo and P.-Y. Chen, "A low-cost wide-angle coverage rectennas for energy harvesting applications," 2023.
- [5] Y. W. L. L. Hao Yi, "A Novel Broadband Micro strip Patch Antenna with Small Ground Plane," p. 3, 2018.
- [6] A. M. S. Viana, S. T. M. Gonçalves, U. C. Resende and T. H. G. Mello, "Dual Band Analysis of a Novel Rectenna for Wireless Power Transmission and Energy Harvesting Applications," no. 05 July 2024, 2024.
- [7] A. OKBA, A. TAKACS and H. AUBERT, "Compact Flat Dipole Rectenna for Energy Harvesting or Wireless Power Transmission Applications," no. 13 January 2019, 2018.
- [8] S. D. Joseph, H. S. S. H. and Y. Huang, "Rectennas for Wireless Energy Harvesting and Power Transfer," no. 15 October 2021, 2021.
- [9] A. Sidibe, G. Loubet, A. Takacs and D. Dragomirescu, "Energy Harvesting for Battery-Free Wireless Sensors Network Embedded in a Reinforced Concrete Beam," no. 02 February 2021, 2021.
- [10] M. Sansoy, A. S. Buttar and R. Goyal, "Empowering Wireless Sensor Networks with RF Energy Harvesting," p. 5, 2020.
- [11] T. Maruyama, K. Shibata, T. Kimura and M. Nakatsugawa, "Extension of WPT Distance for Folded Dipole Rectenna by Using Parasitic Elements as Directors," p. 6, 2022.
- [12] M. H. R. S. K. P. M. T. A. Jahidul Islam Md. Mahfuzur Rahman, "Wireless Power Transmission Circuit and System," *IEEE*, p. 5, 2024.